BIOCHEMISTRY
including biophysical chemistry & molecular biology
Article

Biochemistry **2010,** *49,* 635–644 635
DOI: 10.1021/bi901779p

Residues Essential for Plasminogen Binding by the Cation-Independent Mannose 6-Phosphate Receptor†

Richard N. Bohnsack, Manish Patel, Linda J. Olson, Sally S. Twining, and Nancy M. Dahms*

Department of Biochemistry, Medical College of Wisconsin, Milwaukee, Wisconsin 53226

Received October 15, 2009; Revised Manuscript Received December 21, 2009

ABSTRACT: The 300 kDa cation-independent mannose 6-phosphate receptor (CI-MPR) is a multifunctional protein that binds diverse intracellular and extracellular ligands with high affinity. The CI-MPR is a receptor for plasminogen, and this interaction can be inhibited by lysine analogues. To characterize the molecular basis for this interaction, surface plasmon resonance (SPR) analyses were performed using truncated forms of the CI-MPR and plasminogen. The results show that the N-terminal region of the CI-MPR containing domains 1 and 2, but not domain 1 alone, of the receptor's 15-domain extracytoplasmic region binds plasminogen ($K_d = 5 \pm 1$ nM) with an affinity similar to that of the full-length receptor ($K_d = 20 \pm 6$ nM). In addition to its C-terminal serine protease domain, plasminogen contains lysine binding sites (LBS), which are located within each of its five kringle domains, except kringle 3. We show that kringles 1−4, but not kringles 1−3, bind the CI-MPR, indicating an essential role for the LBS in kringle 4 of plasminogen. To identify the lysine residue(s) of the CI-MPR that serve(s) as an essential determinant for recognition by the LBS of plasminogen, site-directed mutagenesis studies were carried out using a construct encoding the N-terminal three domains of the CI-MPR (Dom1−3His) which contains both a mannose 6-phosphate (Man-6-P) and plasminogen binding site. The results demonstrate two lysine residues (Lys53 located in domain 1 and Lys125 located in the loop connecting domains 1 and 2) of the CI-MPR are key determinants for plasminogen binding but are not required for Man-6-P binding.

Plasminogen, the precursor of the serine protease plasmin and the antiangiogenic molecules, the angiostatins, is synthesized by liver and extrahepatic cells as a 92 kDa glycoprotein. It is a key component of the plasminogen activation system that is important in fibrinolysis, cell migration, tissue remodeling, inflammation, and tumor cell invasion. Glu-plasminogen, the full-length form of plasminogen, consists of seven domains: an N-terminal PAN (plasminogen/apple/nematode) module, five kringle domains (K1−K5), and a C-terminal serine protease domain with trypsin-like activity (*1*, *2*). The kringle domains, each ~80 residues in length, share a common double-loop disulfide structure and are responsible for plasminogen binding to extracellular matrix proteins by the lysine binding site (LBS)[1] found in some (K1, K2, K4, and K5, with K2 and K5 exhibiting the weakest binding), but not all (K3), of the kringle domains (*3*−*6*). Plasminogen is converted to plasmin, a two-chain active serine protease, by an initial cleavage at the Lys77−Lys78 bond releasing the PAN module and exposing the Arg561−Val562 peptide bond, which is cleaved by specific plasminogen activators. Plasminogen can be activated by different proteases, but its specific physiological activators are tissue-type plasminogen activator (tPA) and urokinase-type plasminogen activator (uPA), both of which are serine proteases (*2*). Plasminogen also serves as the precursor of angiostatins, which are a group of proteolytic products of plasminogen containing at least one intact kringle domain but lacking the protease domain. Angiostatins function as potent inhibitors of vascular endothelial cell proliferation, migration, and tube formation and induce endothelial cell apoptosis (*7*). Furthermore, kringles 1−3, 1−4, 1−5, and 2−3, as well as single kringles except for kringle 4, have been shown to possess antiangiogenic activity (*8*−*11*).

The plasminogen activation system is regulated by numerous activators, inhibitors, and receptors (*2*, *12*, *13*). One of these receptors is the 300 kDa cation-independent mannose 6-phosphate receptor (CI-MPR), a multifunctional protein that binds a number of different ligands including (1) a carbohydrate moiety, mannose 6-phosphate (Man-6-P) found on N-linked glycans of lysosomal enzymes (*14*) and selected growth factors (e.g., latent transforming growth factor-β (TGF-β) (*15*)), (2) insulin-like growth factor II (IGF-II) (*16*), (3) retinoic acid (*17*), (4) urokinase-type plasminogen activator receptor (uPAR) (*18*), and (5) plasminogen (*19*). The ability of the CI-MPR to interact with so many different molecules is facilitated by the receptor's large (~2270 amino acids) extracytoplasmic region comprising 15 homologous domains, which have a similar size (~150 residues), conservation of residues, and spacing of conserved cysteine residues (six or eight cysteines) involved in disulfide bonding. In addition, the crystal structure of 7 (i.e., domains 1−3, domains 11−14) out of the 15 domains of the CI-MPR has been determined to date, which shows that each of these domains shares a similar fold (*20*−*22*). Several distinct ligand binding sites have been localized to individual domains: the three Man-6-P binding sites are localized to domains 3, 5, and 9 (*23*, *24*); the

†This work was supported in part by National Institutes of Health Grants R01DK42667 (to N.M.D.) and R01EY012731 (to S.S.T.).

*Address correspondence to this author. Tel: 414-955-4698. Fax: 414-955-6510. E-mail: ndahms@mcw.edu.

[1]Abbreviations: Glu-plasminogen, full-length plasminogen with an intact N-terminal PAN module; LBS, lysine binding site; tPA, tissue-type plasminogen activator; uPA, urokinase-type plasminogen activator; CI-MPR, cation-independent mannose 6-phosphate receptor; Man-6-P, mannose 6-phosphate; TGF-β, transforming growth factor-β; IGF-II, insulin-like growth factor II; uPAR, urokinase-type plasminogen activator receptor; SPR, surface plasmon resonance; sCI-MPR, soluble form of the CI-MPR isolated from fetal bovine serum; Ni-NTA, nickel nitriloacetic acid; AHA, 6-aminohexanoic acid.

Published on Web 12/22/2009

IGF-II binding site has been mapped to domain 11, with residues in domain 13 increasing the affinity of the interaction by ~10-fold (*25*, *26*); residues important for plasminogen and uPAR binding appear to reside in domain 1 (*27*); the location of the retinoic acid binding site has not yet been determined (Figure 1).

A growing body of evidence supports the CI-MPR's role in activating TGF-β, which involves the receptor's association with plasminogen (*15*, *19*, *27*−*32*). TGF-β is secreted as an inactive complex, termed latent TGF-β. Inactive latent TGF-β, which contains the Man-6-P tag, binds to the CI-MPR at the cell surface (*15*). A model has been presented in which the CI-MPR serves as a platform to facilitate the proteolytic cleavage of latent TGF-β, thereby generating the biologically active form of this growth factor: the CI-MPR directly binds uPAR, plasminogen, and latent TGF-β; uPA bound to uPAR converts plasminogen to plasmin, which in turn proteolytically activates latent TGF-β (*32*). The CI-MPR has also been reported to alter the subcellular distribution of uPAR by directing it to the lysosome for degradation (*18*), analogous to its established role in regulating the activity of IGF-II by receptor-mediated endocytosis and subsequent delivery of this growth factor to the lysosome for degradation (*33*, *34*). Thus, the possibility exists that the CI-MPR may also function in specific cell types to internalize and deliver plasminogen/plasmin to the lysosome.

Given the complexity of interactions that the CI-MPR can undergo at the cell surface, some of which impact growth factor activity, an understanding of the molecular basis governing these interactions is needed to reveal the mechanisms involved in regulating these processes. In the current study, site-directed mutagenesis and surface plasmon resonance (SPR) analyses were performed to probe the molecular basis of the interaction between plasminogen and the CI-MPR. The results demonstrate Lys53 and Lys125 of the CI-MPR are key determinants for plasminogen binding. Furthermore, the LBS in kringle 4 of plasminogen plays an essential role in this interaction as the plasminogen fragment containing kringles 1−3 exhibits no detectable binding to the CI-MPR, whereas kringles 1−4 bind the CI-MPR with an affinity similar (within 2.3-fold) to that of full-length plasminogen.

EXPERIMENTAL PROCEDURES

Reagents. Purified bovine and human plasminogen and bovine and human prothrombin were purchased from Haematological Technologies, Inc., and dialyzed exhaustively against either HBS buffer (50 mM HEPES, pH 7.5, 150 mM NaCl) or HBA buffer (50 mM HEPES, pH 7.5, 150 mM sodium acetate). IGF-II was purchased from Cell Sciences Inc. Recombinant human angiostatin K1−3 and human angiostatin K1−4 were purchased from Calbiochem and Haematological Technologies, Inc., respectively. Human and bovine prothrombin (Haematologic Technologies, Inc.; contains two kringle domains and was purified from plasma) and human urokinase-type plasminogen activator (uPA; Calbiobiochem; contains one kringle domain and was isolated from human urine) were purchased as indicated.

Purification of Soluble CI-MPR from Fetal Bovine Serum. A soluble form of the CI-MPR (sCI-MPR) was purified from fetal bovine serum by phosphomannan affinity chromatography as described previously (*35*).

Generation of CI-MPR Constructs Encoding Domain 1 and Domains 1 and 2. Previously generated cDNA construct encoding extracytoplasmic domains 1−3 (Dom1−3His) of the

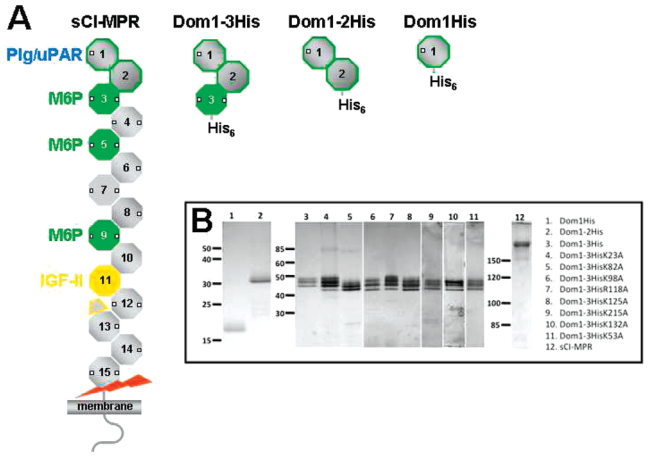

FIGURE 1: MPR constructs. (A) Schematic diagram of sCI-MPR, Dom1−3His, Dom1−2His, and Dom1His constructs. Based on its size, the sCI-MPR is predicted to contain most of the extracellular region (i.e., extracellular domains 1−15). However, the site of cleavage (red arrow) is not known and could occur within domain 15. The small white squares indicate potential N-glycosylation sites. The location of the ligand binding sites is shown. Domains 1 and 2 are outlined in green since the presence of these two domains enhances the affinity of domain 3 for lysosomal enzymes by ~1000-fold (*24*). (B) SDS−polyacrylamide gel of sCI-MPR purified from bovine serum and Dom1−3His, Dom1−2His, and Dom1His constructs purified from the medium of transformed *P. pastoris* yeast. The proteins are visualized by silver staining. The multiple bands observed for Dom1−3His are due to differences in the utilization of the three N-glycosylation sites as determined by enzymatic deglycosylation using endo-β-*N*-acetylglucosaminidase H digestion (data not shown).

bovine CI-MPR followed by a C-terminal tag of six histidine residues (*36*) was used as a PCR template to generate constructs encoding either domain 1 (Dom1His) or domains 1 and 2 (Dom1−2His) followed by a C-terminal His_6 tag. Briefly, the sequence encoding domain 1 (residues 1−123) followed by six histidine residues (CAC) and a stop codon (TGA) was amplified by PCR and subcloned into the *Pichia pastoris* expression vector pGAPZαA (Invitrogen) using the *Xho*I (5′ end) and *Xba*I (3′ end) restriction sites of the pGAPZαA vector. The sequence encoding domains 1−2 (residues 1−281) followed by six histidine residues (CAC) and a stop codon (TGA) was amplified by PCR and cloned into Dom1−3His pGAPZαA using an internal *Ban*I site and *Xba*I (3′ end). DNA sequencing by the Protein and Nucleic Acid Core Facility (Medical College of Wisconsin) confirmed the predicted sequences.

Expression and Purification of CI-MPR Constructs. Dom1−3His (residues 1−432 of the bovine CI-MPR), Dom1−2His (residues 1−281 of the bovine CI-MPR), and Dom1His (residues 1−123 of the bovine CI-MPR) cDNA constructs were linearized with *Bsp*HI and transformed into *P. pastoris* wild-type strain X-33 (Invitrogen) by electroporation, and zeocin-resistant transformants were selected as described previously (*37*). These constructs, which use the promoter from the glyceraldehyde 3-phosphate dehydrogenase gene for constitutive protein expression, are engineered in-frame with the 89-residue *Saccharomyces cerevisiae* α-factor signal sequence, resulting in proteins that are secreted from *P. pastoris*. Positive clones were inoculated in liquid medium (1% yeast extract, 2% peptone, and 2% dextrose), and cultures were harvested after 3 days of growth at 30 °C. Following removal of the cells by centrifugation, the medium was dialyzed against nickel binding buffer (20 mM Tris and 500 mM NaCl, pH 8.0). The dialyzed medium was

passed over a nickel nitrilotriacetic acid (Ni-NTA) agarose (Qiagen) column, washed, and then eluted with nickel binding buffer containing 100 mM imidazole. Purified Dom1−3His, Dom1−2His, Dom1His, and Dom1−3His mutants were extensively dialyzed against either HBS or HBA buffer and concentrated by filtration using a 4 mL Vivaspin spin column. The Bradford protein assay (Bio-Rad) with bovine serum albumin as the standard was used to estimate protein yields.

Site-Directed Mutagenesis of the CI-MPR (Domains 1−3). Mutant Dom1−3His cDNAs were generated using the QuickChange mutagenesis kit from Stratagene. DNA sequencing by the Protein and Nucleic Acid Core Facility (Medical College of Wisconsin) confirmed the predicted sequences.

Purification of Human β-Glucuronidase. Human β-glucuronidase was collected from serum-free conditioned medium from cells that overexpress and secrete this lysosomal enzyme (MTX 3.2 cells were generously provided by Dr. William Sly, St. Louis University School of Medicine, St. Louis, MO). β-Glucuronidase was purified by affinity chromatography on a CI-MPR Affi-Gel-10 column to remove nonphosphorylated enzyme as described previously (*38*).

Biosensor Studies. All SPR measurements were performed at 25 °C using a Biacore 3000 instrument (BIAcore; GE Healthcare). CM5 research grade sensor chips, surfactant P20, and amine coupling kits were also obtained from BIAcore. Purified proteins (sCI-MPR, Dom1−3His, Dom1−2His, Dom1-His, Dom1−3His mutants, and plasminogen) were immobilized on CM5 sensor chips following activation of the surface using 1-ethyl-3-(3-dimethylaminopropyl)carbodiimide and *N*-hydroxysuccinimide as recommended by the manufacturer. Briefly, the proteins were injected onto the activated dextran surface at a concentration of 10−20 μg/mL in 10 mM sodium acetate buffer, pH 5.0, using 10 mM HEPES, pH 7.5, 150 mM NaCl, and 0.005% (v/v) P20 as the running buffer. After coupling, unreacted *N*-hydroxysuccinimide ester groups were blocked with ethanolamine. The reference surface was treated in the same way except that protein was omitted. Samples of purified proteins β-glucuronidase, IGF-II, uPA, prothrombin, angiostatin K1−3, angiostatin K1−4, or plasminogen were prepared in HBS or HBA supplemented with 0.005% (v/v) P20 and were injected in a volume of 80 μL over the coupled and reference flow cells at a flow rate of 40 μL/min. After 2 min, the solutions containing the purified proteins were replaced with buffer, and the complexes were allowed to dissociate for 2 min. The sensor chip surface was regenerated with a 20 μL injection of 10 mM 6-aminohexanoic acid (AHA) for kringle-containing proteins at a flow rate of 10 μL/min, 10 mM Man-6-P for β-glucuronidase at a flow rate of 10 μL/min, or 10 mM HCl for IGF-II at a flow rate of 10 μL/min. The surface was allowed to reequilibrate in running buffer for 1 min prior to subsequent injections. The response at equilibrium (R_{eq}) for each concentration of protein was determined by averaging the response over a 10 s period within the steady-state region of the sensorgram using the BIAevaluation software package (version 4.0.1). The response at equilibrium (R_{eq}) was plotted versus the concentration of protein and fit by nonlinear regression to a one-site saturation-binding model using the equation $y = (R_{max}[MPR])/(K_d + [MPR])$ (SigmaPlot version 10.0; Systat Software, Inc.). A two-site saturation binding model using the equation $y = (R_{max_1}[MPR]/(K_{d1} + [MPR]) + R_{max_2}[MPR]/(K_{d2} + [MPR])$ (SigmaPlot version 10.0; Systat Software, Inc.) was used when evaluating plasminogen binding at high concentrations (>120 nM). All response data were double referenced (*39*), where controls for the contribution of the change in refractive index were performed in parallel with flow cells derivatized in the absence of protein and subtracted from all binding sensorgrams.

RESULTS

The N-Terminal Region of the CI-MPR Binds Lysosomal Enzymes and Plasminogen with the Same Affinity as the Soluble CI-MPR (sCI-MPR) Isolated from Serum. To analyze the interaction between the CI-MPR and plasminogen, surface plasmon resonance (SPR) studies were performed on well-characterized forms of the CI-MPR. We compared the ∼260 kDa soluble form of the CI-MPR (sCI-MPR) found in serum and extracellular fluids, which contains much of the extracytoplasmic region and has been shown to bind Man-6-P-containing lysosomal enzymes and IGF-II (*40*−*43*), and a construct encoding the receptor's N-terminal region (domains 1−3) (Figure 1A). This Dom1−3His construct, which contains a C-terminal His tag, has been studied extensively in our laboratory: we have determined its crystal structure (*20*, *44*), and we have shown it contains a high-affinity Man-6-P binding site (*24*, *36*). Ni-NTA affinity chromatography and phosphomannan affinity chromatography were used to purify Dom1−3His and sCI-MPR, respectively, to apparent homogeneity, with the multiple bands representing differing utilization of the three N-linked glycosylation sites (Figure 1B and data not shown). To carry out the SPR analyses, sCI-MPR and Dom1−3His were immobilized on separate flow cells of a CM5 sensor chip, and various concentrations of the Man-6-P-containing lysosomal enzyme β-glucuronidase or IGF-II were flowed over the surface. The results show that sCI-MPR bound both IGF-II (K_d = 1 nM; Figure 2A) and β-glucuronidase (K_d = 22 ± 3 nM; Figure 2B and Table 1) with affinities similar to that reported in the literature (*16*, *45*, *46*). In addition, Dom1−3His bound β-glucuronidase with affinities similar to that of the sCI-MPR isolated from bovine serum (K_d = 10 ± 2 nM; Figure 2C and Table 1) and identical to affinities that we have reported for this construct using a solution-based binding assay and iodinated β-glucuronidase (*24*). As expected, the interaction between the MPRs and β-glucuronidase is inhibited by Man-6-P (insets to Figure 2B,C). These results show that immobilization of sCI-MPR or a truncated version of the receptor (Dom1−3His) to a sensor chip has no significant adverse affects to its binding properties, thus demonstrating the validity of SPR methodology to assess the ligand binding properties of the CI-MPR.

SPR analyses were also conducted on the immobilized sCI-MPR and Dom1−3His constructs in which increasing concentrations of Glu-plasminogen (full-length plasminogen with an intact N-terminal PAN module) were flowed over the sensor chip surface. The results demonstrate that sCI-MPR and Dom1−3His bind Glu-plasminogen with similar affinities (K_{d1} = 20 ± 6 nM versus K_{d1} = 3 ± 1 nM; Table 1). Furthermore, the interaction between sCI-MPR (K_i = 29 ± 1.3 μM) or Dom1−3His (K_i = 26 ± 1.0 μM) and Glu-plasminogen was inhibited to a similar extent by the lysine analogue, 6-aminohexanoic acid (AHA) (Figure 3).

Taken together, these results demonstrate that the construct encoding the N-terminal three domains of the CI-MPR is fully functional: Dom1−3His contains both an intact Man-6-P binding site and an intact plasminogen binding site that exhibit affinities similar to that observed for the sCI-MPR. These data

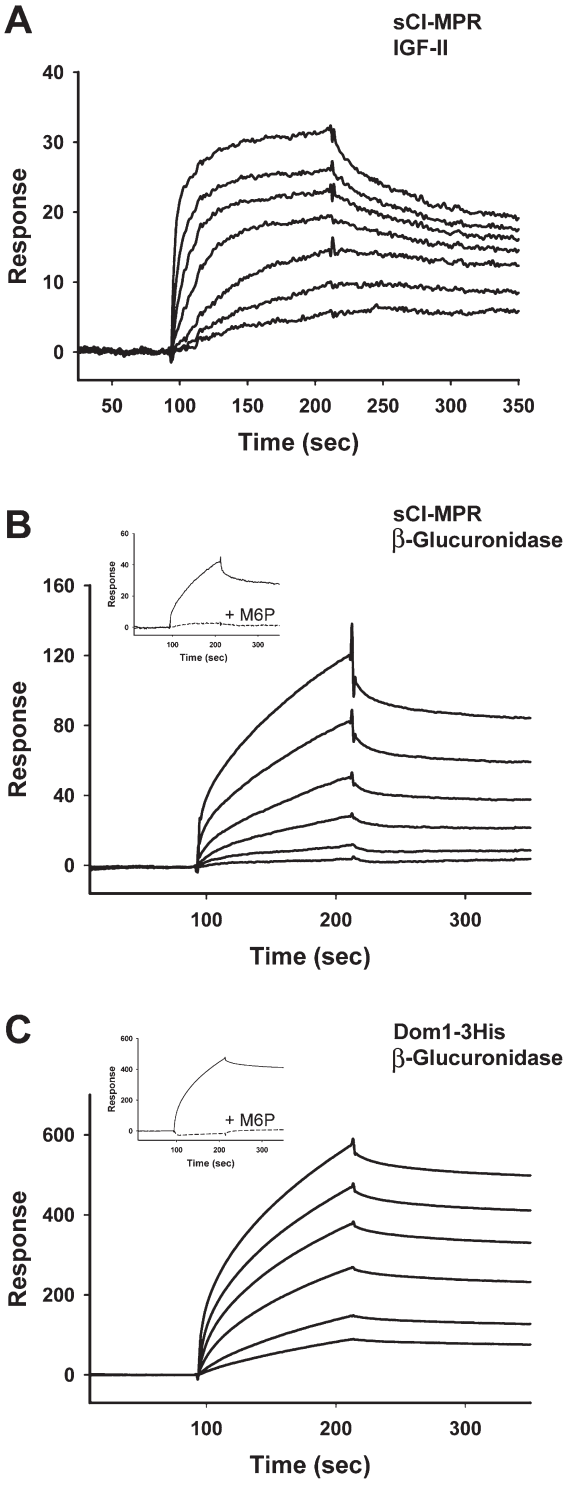

FIGURE 2: Sensorgrams measuring the interaction between the MPRs (sCI-MPR or Dom1−3His) and IGF-II or a lysosomal enzyme. The sCI-MPR and Dom1−3His proteins were coupled to separate flow cells of a CM5 sensor chip, with a final coupling level of 2600 and 1000 response units (RU), respectively. Increasing concentrations of IGF-II or the lysosomal enzyme, β-glucuronidase, were injected onto the chip. (A) Sensorgrams show the interaction between the sCI-MPR and IGF-II (1, 2.5, 5, 10, 25, 50, and 100 nM). (B) Sensorgrams depict the interaction between β-glucuronidase (0.5, 1, 2.5, 5, 10, 25, 50, and 100 nM) and the sCI-MPR or (C) Dom1−3His. The insets in panels B and C are sensorgrams showing the interaction between β-glucuronidase (50 nM) and sCI-MPR or Dom1−3His, respectively, in the absence or presence of 10 mM Man-6-P.

Table 1: Comparison of Binding Affinities of the sCI-MPR and Constructs Containing the N-Terminal Region of the CI-MPR[a]

	plasminogen		
construct	K_{d1} (nM)	K_{d2} (nM)	β-glucuronidase K_d (nM)
sCI-MPR	20 ± 6	290 ± 350	22 ± 3
Dom1His	> 2 μM	> 2 μM	ND
Dom1−2His	5 ± 1	170 ± 50	ND
Dom1−3His	3 ± 1	150 ± 30	10 ± 2

[a]ND: no detectable response. A two-site binding model was used to fit the data for the interaction between plasminogen and the receptor.

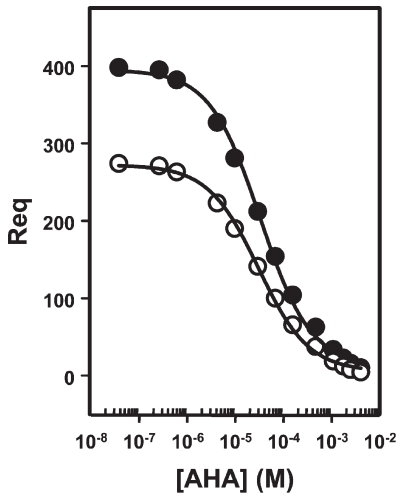

FIGURE 3: 6-Aminohexanoic acid (AHA) inhibits the interaction between Glu-plasminogen and the sCI-MPR or Dom1−3His. SPR analyses were used to estimate the half-maximal inhibition of sCI-MPR (●) and Dom1−3His (○) binding to Glu-plasminogen by AHA. Briefly, Glu-plasminogen was diluted to 25 nM and mixed with increasing concentrations of AHA (0, 0.1, 0.5, 1, 5, 10, 25, 50, 100, 250, 500, 750, 1000, and 1500 μM), and the samples were injected onto the coupled flow cells. The response at equilibrium (R_{eq}) was determined and plotted against the log of the AHA concentration. The K_i (sCI-MPR $K_i = 29 \pm 1.3\,\mu$M; Dom1−3His $K_i = 26 \pm 1.0\,\mu$M) was determined by nonlinear regression using Sigmaplot (version 10.0; Systat Software, Inc.).

also validate the use of this construct (Dom1−3His) for mutational studies as amino acid substitutions made in the context of the Dom1−3His construct can be evaluated for their effect on plasminogen binding as well as for their effect on Man-6-P binding. Thus, the results obtained from probing these two binding sites will be used to evaluate whether a particular mutation has a specific effect on ligand binding or imparts an overall global effect on the protein that is evidenced by an inhibitory impact on both ligand binding sites.

The Conformation of Glu-Plasminogen Influences Its Interaction with the CI-MPR. Glu-plasminogen can assume at least three different conformations as assessed by small-angle X-ray scattering (*47*). At physiological concentrations of NaCl, Glu-plasminogen exists in a "closed" α-conformation, with the PAN module bound to kringle 5, which displays a radius of gyration of 30.7 Å. In the presence of benzamidine, Glu-plasminogen is in the intermediate β-conformation and displays a radius of gyration of 42.1 Å. In the presence of AHA (mimic of protein lysine residues), Glu-plasminogen undergoes a dramatic change in conformation resulting in an extended ("open"), flexible γ-conformation with a radius of gyration of 50.3 Å. In

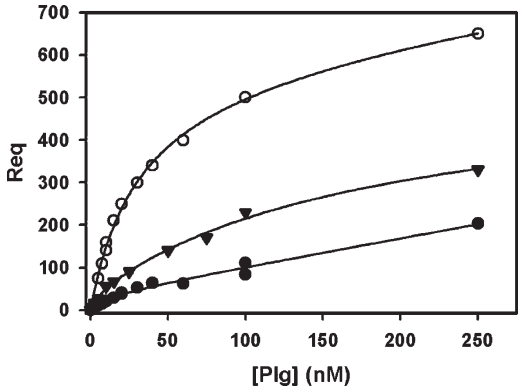

FIGURE 4: The conformation of Glu-plasminogen influences its interaction with the CI-MPR. Aliquots containing 2.5, 5, 7.5, 10, 15, 20, 30, 40, 60, 100, and 250 nM bovine Glu-plasminogen in HBA buffer containing 150 mM sodium acetate, pH 7.4 (○), or HBS buffer containing 150 mM NaCl, pH 7.4 (●), or aliquots containing 1, 2.5, 5, 10, 15, 25, 50, 75, 100, and 250 nM Glu-plasminogen in HBA buffer with 50 mM benzamidine (▼) were injected onto a Dom1−3His-coupled CM5 sensor chip. The response at equilibrium (R_{eq}) was determined and plotted against the concentration of Glu-plasminogen ([Plg]). The data were fit by nonlinear regression using a two-site saturation binding model.

the presence of acetate ions, but without chloride ions, Glu-plasminogen is also in an open conformation, but not to the extent observed in the presence of AHA (*48*). Our previous work showed that these various conformations also affect the ability of proteases to generate the kringle-containing antiangiogenic molecules, angiostatins, from plasminogen: neutrophil elastase more readily converted Glu-plasminogen to angiostatins in the presence of benzamidine or acetate ions than in the presence of NaCl (*49*). SPR analyses demonstrate that the conformational state of Glu-plasminogen affects significantly the affinity of its interaction with Dom1−3His: the closed α-conformation of Glu-plasminogen binds with the lowest affinity to the receptor (K_d = 271 ± 80 nM); the intermediate β-conformation binds with an intermediate affinity (K_d = 131 ± 16 nM); in the presence of acetate ions, the open γ-conformation binds with the highest affinity (K_d = 20 ± 6 nM) (Figure 4). The K_d obtained in the closed conformation in the presence of physiological levels of NaCl is the same as that reported by Leksa et al. (K_d = 270 nM) (*32*) under similar normal saline conditions.

Kringle 4 of Plasminogen Is Required for High-Affinity Binding to the CI-MPR. Angiostatins (plasminogen kringle domains 1−3 (K1−3), K1−4, K1−5, and single kringle domains other than K4), a group of antiangiogenic molecules, are usually generated by cleavage of plasminogen in the linker regions between kringle domains (*8*, *9*, *11*). To determine whether angiostatins are capable of interacting with the CI-MPR, the angiostatins K1−3 and K1−4 were analyzed for their ability to bind Dom1−3His. Prior to these experiments, a control was performed to evaluate whether species-specific differences exist that impact binding affinities between the CI-MPR and plasminogen, as the bovine sCI-MPR and its truncated forms are used in this study. The results show that Dom1−3His of the CI-MPR binds bovine and human Glu-plasminogen with similar affinity (within 2.3-fold), demonstrating that human and bovine Glu-plasminogen do not differ appreciably in their ability to recognize the bovine CI-MPR (Table 2). In contrast to the full-length plasminogen, no detectable binding was observed between Dom1−3His and human angiostatin K1−3 at various concentrations of K1−3 up to and including 500 nM. However, a robust interaction was observed between human angiostatin K1−4 and Dom1−3His, with the affinity (K_d = 170 ± 50 nM) only ~2.4-fold lower than that observed with human Glu-plasminogen (Table 2). To determine whether nonplasminogen kringle-containing proteins are capable of interacting with the N-terminal region of the CI-MPR, human urokinase-type plasminogen activator (uPA, contains one kringle domain) and human and bovine prothrombin (contains two kringle domains) were evaluated. The SPR analyses demonstrate that uPA and prothrombin exhibit no significant interaction with Dom1−3His (Table 2). Together, these results demonstrate that kringle 4 of plasminogen is essential for high-affinity interaction with the N-terminal region of the CI-MPR. Furthermore, not all kringle domains are capable of interacting with the CI-MPR, as other kringle-containing proteins (e.g., angiostatin K1−3, uPA, and prothrombin) exhibit no specific binding to the receptor.

Table 2: Summary of Binding Affinities for the Interaction of the N-Terminal Region of the CI-MPR with Kringle-Containing Proteins[a]

kringle-containing protein	K_d (nM)
bovine plasminogen	30 ± 2
human plasminogen	70 ± 10
human plasminogen K1−4	170 ± 50
human plasminogen K1−3	ND
human uPA	ND
human prothrombin	>2.5 μM
bovine prothrombin	>2.5 μM

[a]ND: no detectable response was observed for K1−3 (500 nM) or uPA (100 nM).

Domains 1 and 2 of the CI-MPR Are Required for Its Interaction with Plasminogen. Based on our crystal structure of domains 1−3 of the CI-MPR (*20*) and the analysis of truncation mutants of the CI-MPR by Leksa et al. (*27*), we proposed that the plasminogen binding site is located in a cleft formed by the interface between domains 1 and 2 of the CI-MPR which contains several surface lysine residues (Figure 5). Consistent with this hypothesis, we have demonstrated that a construct encoding domains 1 and 2 of the CI-MPR (Dom1−2His; Figure 1B) binds Glu-plasminogen with a similar affinity as Dom1−3His (K_{d1} = 5 ± 1 nM and K_{d1} = 3 ± 1 nM, respectively; Figure 6 and Table 1). In contrast, no specific binding was detected to Dom1His (Figure 1B) at concentrations of Glu-plasminogen up to and including 2 μM (Figure 6 and data not shown). The crystal structure of domains 1−3 of the CI-MPR revealed that each domain has a similar overall fold: a flattened β-barrel consisting of two antiparallel β-sheets, one with four β-strands and the other with five β-strands (*20*) (Figure 5). Analysis of Dom1His by circular dichroism spectroscopy demonstrated that the protein is folded, exhibiting significant secondary structure consistent with a protein comprised of predominantly β-strands (Supporting Information Figure 1A). Furthermore, Dom1His protein exists entirely as a monomer as assessed by gel filtration (Supporting Information Figure 1B). Thus, the lack of detectable interaction between Dom1His and Glu-plasminogen is not due to either misfolding or aggregation of the Dom1His protein. Taken together, the results show that the N-terminal two domains of the CI-MPR are required for high-affinity binding by Glu-plasminogen.

Lysine Residues at Positions 53 and 125 of the CI-MPR Are Key Determinants Recognized by Glu-Plasminogen. To probe which surface lysine residue(s) of the CI-MPR are

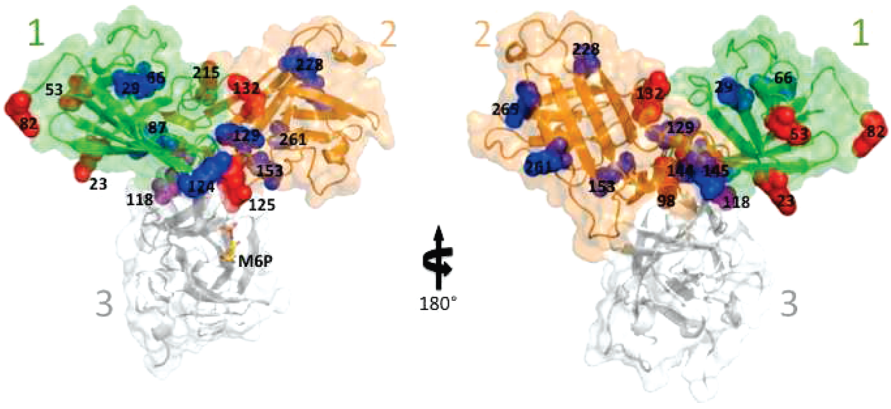

FIGURE 5: Location of lysine residues in domains 1−3 of the CI-MPR. A ribbon diagram overlaid with a transparent surface model of the crystal structure of domains 1−3 of the CI-MPR (PDB accession number 1SZ0) is shown. The view in the right panel is rotated 180° from that shown in the left panel. The side chains of all lysine residues in domain 1 (green) and domain 2 (orange) are shown in blue, and the lysine residues that have been mutated are indicated in red. Arg118 is highlighted in purple. The bound Man-6-P in domain 3 (gray) is also shown (yellow ball-and-stick representation). The figure was generated using PyMOL (*60*).

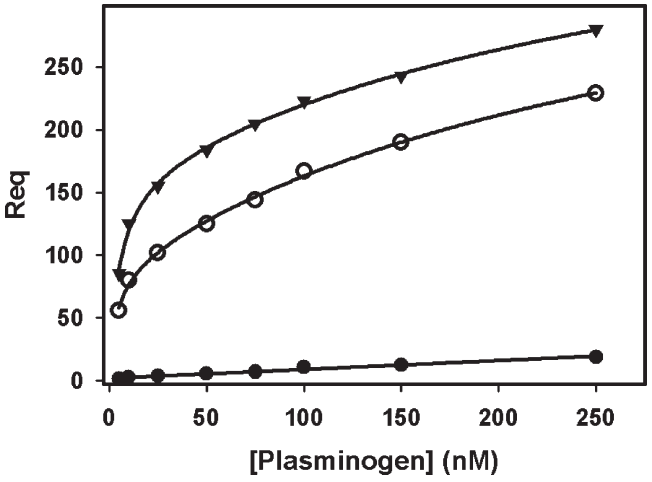

FIGURE 6: Domain 3 of the CI-MPR is not required for the receptor's interaction with Glu-plasminogen. Aliquots containing 10, 25, 50, 75, 100, 150, and 250 nM bovine Glu-plasminogen in HBA buffer containing 150 mM sodium acetate, pH 7.4, were injected onto CM5 sensor chips containing coupled Dom1−3His (○), Dom1−2His (▼), or Dom1His (●). The response at equilibrium (R_{eq}) was determined and plotted against the concentration of Glu-plasminogen ([Plg]). The data were fit by nonlinear regression using a two-site saturation binding model.

essential for binding by Glu-plasminogen, selected lysine residues of Dom1−3His were replaced with alanine. The purified constructs were immobilized to separate flow cells of CM5 sensor chips, and the binding affinity to Glu-plasminogen and the lysosomal enzyme β-glucuronidase was determined. The results are summarized in Table 3. Because Dom1−2His bound Glu-plasminogen with an affinity similar to that of Dom1−3His (Figure 6), lysine residues within domain 3 were not evaluated. Furthermore, surface-exposed lysine residues in domain 1 and 2, as revealed by the crystal structure of domains 1−3 (*20*, *44*), were chosen for mutagenesis (Figure 5). Although our results showed that a construct encoding domain 1 alone exhibited no significant binding to Glu-plasminogen (Figure 6), previous studies by Leksa et al. (*27*) showed that a mutant human CI-MPR construct containing the N-terminal two-thirds of domain 1 fused to the transmembrane and cytosolic region of the receptor bound to plasminogen coated on wells of a 96-well plate. To address this observation and to further evaluate the possible role of the

Table 3: Summary of Binding Affinities for the Interaction of CI-MPR Constructs with Plasminogen and β-Glucuronidase

	K_d	
construct	plasminogen	β-glucuronidase
Dom1−3His	35 ± 6	10 ± 2
Dom1−3HisK23A	33 ± 7	14 ± 1
Dom1−3HisK53A	> 2 μM	17 ± 2
Dom1−3HisK82A	69 ± 11	17 ± 2
Dom1−3HisK98A	24 ± 5	17 ± 1
Dom1−3HisR118A	21 ± 5	12 ± 1
Dom1−3HisK125A	> 2 μM	26 ± 2
Dom1−3HisK132A	64 ± 9	35 ± 4
Dom1−3HisK215A	10 ± 1	18 ± 2

CI-MPR's N-terminal region in plasminogen binding, our initial studies focused on surface-exposed lysine residues of domain 1: of the seven lysine residues in domain 1, only three at positions 23, 53, and 82 are significantly solvent exposed (Figure 5). The results show that the K23A mutant binds β-glucuronidase and Glu-plasminogen with similar affinities as the wild-type Dom1−3His (Table 3), whereas replacement of lysine at position 82 resulted in a minimal (2-fold) decrease in affinity toward Glu-plasminogen with no significant change in the recognition of β-glucuronidase (Table 3). In contrast, while the K53A mutant bound β-glucuronidase with an affinity similar to that of the wild-type Dom1−3His, its interaction with Glu-plasminogen was dramatically inhibited, with little specific binding observed even at high concentrations (2 μM) of Glu-plasminogen (Table 3, Figures 7 and 8). As a control, we also assessed whether hydrogen- bonding interactions between domain 1 and domain 3 serve an essential role in ligand binding. Lys98, which interacts with the backbone carbonyls of Val417 and Asp418 in domain 3 and is buried in the structure (Figure 5), was replaced with alanine. The results show that the K98A mutant binds β-glucuronidase and Glu-plasminogen with a similar affinity as the wild-type Dom1−3His (Table 3), demonstrating that this interdomain interaction is not essential for high-affinity binding of either plasminogen or Man-6-P-containing ligands.

The cleft formed by the interface between domains 1 and 2 of the CI-MPR contains surface lysine residues at positions 132 and 215, both of which are located in domain 2 (Figure 5). To determine whether these residues play a role in plasminogen

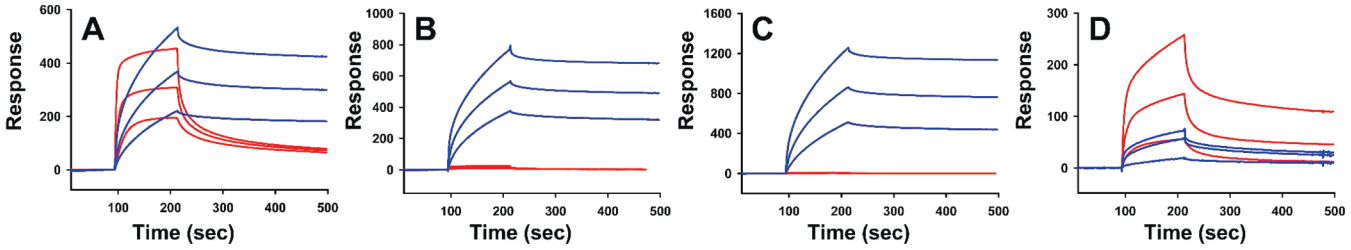

FIGURE 7: SPR analyses of wild-type and mutant Dom1−3His construct interaction with Glu-plasminogen or β-glucuronidase. Similar amounts of Dom1−3His, K53A, K125A, and K132A were immobilized on the surface of a CM5 sensor chip, and increasing concentrations of Glu-plasminogen or β-glucuronidase were injected over the MPR and reference flow cells at a flow rate of 40 μL/min. Shown are representative sensorgrams for (A) Dom1−3His, (B) K53A, (C) K125A, and (D) K132A at three concentrations (10, 40, and 120 nM) of Glu-plasminogen (red lines) or β-glucuronidase (blue lines), with the exception of K132A in which sensorgrams at concentrations of 10, 50, and 100 nM β-glucuronidase are shown.

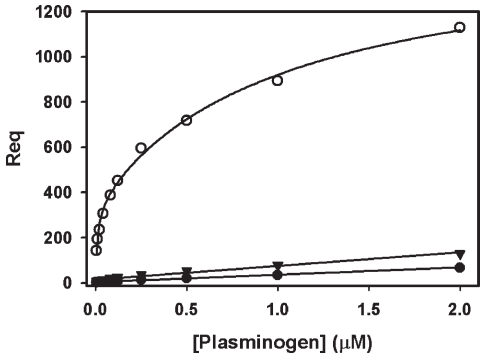

FIGURE 8: Lys53 and Lys125 of the CI-MPR are required for the receptor's interaction with Glu-plasminogen. Aliquots containing 10, 25, 50, 75, 100, 150, and 250 nM bovine Glu-plasminogen in HBA buffer containing 150 mM sodium acetate, pH 7.4, were injected onto CM5 sensor chips containing coupled Dom1−3His (○), K53A (▼), or K125A (●). The response at equilibrium (R_{eq}) was determined from the resulting sensorgrams and plotted against the concentration of Glu-plasminogen ([Plg]). The data were fit by nonlinear regression using a two-site saturation binding model.

binding, single amino acid substitutions were generated in Dom1−3His. The K215A mutant bound β-glucuronidase and Glu-plasminogen with a similar affinity as the wild-type Dom1−3His (Table 3), indicating that Lys215 does not play a significant role in plasminogen binding. In contrast, substitution of lysine at position 132 with alanine had a significant effect on β-glucuronidase binding, affecting both affinity (3.5-fold decrease) and the overall response (~4-fold decrease in R_{max}), and an inhibitory effect on Glu-plasminogen binding (2-fold decrease) (Figure 7 and Table 3). These data suggest that substitution of lysine at position 132 has a global effect on the structure of domains 1−3, resulting in greater inhibitory effect on lysosomal enzyme binding than Glu-plasminogen recognition. Of the remaining exposed lysine residues within domain 2, Lys125, which is located in the loop connecting domains 1 and 2, is highly exposed and interacts with the loop connecting β-strands 6 and 7 of domain 3. The K125A mutant bound β-glucuronidase with a similar affinity as the wild-type Dom1−3His but exhibited a dramatic reduction in its ability to interact with Glu-plasminogen as minimal specific binding was observed at high concentrations of Glu-plasminogen (Table 3 and Figures 7 and 8). As a control, Arg118, which is located at the C-terminal end of domain 1 and also interacts with the loop connecting β-strands 6 and 7 of domain 3, was replaced with alanine. The results show that the R118A Dom1−3His mutant exhibits a similar affinity toward Glu-plasminogen and β-glucuronidase as the wild-type Dom1−3His (Table 3). Taken together, these data demonstrate that Lys53 and Lys125 of the CI-MPR are key determinants for plasminogen binding and suggest both domain 1 and the linker region between domains 1 and 2 are required for stable plasminogen binding.

DISCUSSION

Plasminogen binds the CI-MPR directly, and importantly, this interaction has been shown to facilitate the proteolytic activation of latent TGF-β in several cell types (*19*, *32*). Although this interaction can be inhibited by the lysine analogue, tranexamic acid (*19*), little is known concerning the molecular basis governing the CI-MPR's role as a cell surface receptor for plasminogen. A previous report in which the CI-MPR-containing deletions within the extracytoplasmic region were assayed qualitatively for binding to plasminogen indicated that constructs containing an intact domain 1 or the N-terminal half of domain 1 bound plasminogen-coated, but not BSA-coated, wells of a 96-well plate (*27*). Thus, the authors concluded that the N-terminal region of the CI-MPR is crucial for binding plasminogen. However, on the basis of our crystal structure of domains 1−3 of the CI-MPR (*20*, *44*), we predict that their construct containing the N-terminal half of domain 1 is misfolded as the deletion site occurs within β-strand 6 of domain 1's C-terminal β-sheet, leading to exposure of lysine residues that could serve as docking sites for plasminogen. In the current study, we have conducted quantitative binding studies using the N-terminal region of the CI-MPR truncated in the linker region between domains, plus a construct containing both Man-6-P and plasminogen binding sites that was engineered to have single amino acid substitutions to characterize the interaction between the CI-MPR and plasminogen.

To map the regions of the CI-MPR and plasminogen that are required for high-affinity binding, SPR analyses were carried out on truncated forms of the CI-MPR and plasminogen. Our results demonstrate that constructs encoding the N-terminal three (Dom1−3His) or two domains (Dom1−2His) of the CI-MPR interact with Glu-plasminogen with an affinity similar to that of the CI-MPR, whereas a construct encoding domain 1 alone (Dom1His) exhibits no detectable binding to plasminogen (Table 1 and Figure 6). To determine whether specific lysine residues of the CI-MPR are involved in its interaction with plasminogen, we took advantage of the fact that the N-terminal three domains of the CI-MPR (Dom1−3His) house two functional ligand binding sites, plasminogen and Man-6-P found on lysosomal enzymes (Figures 2 and 3). Thus, the Dom1−3His construct was used to distinguish between those mutations that have a global inhibitory effect on receptor function, impacting

both ligand binding activities of the receptor, versus those that specifically affect the CI-MPR's interaction with plasminogen. The results demonstrate that Lys53 within domain 1 and Lys125 within the loop connecting domains 1 and 2 (Figure 5) of the CI-MPR serve as key determinants for recognition by plasminogen as replacement of either of these lysine residues with alanine ablates plasminogen binding but not the receptor's interaction with a lysosomal enzyme (Table 3 and Figures 7 and 8). Although we cannot rule out that other residues of the CI-MPR participate in plasminogen binding, the results clearly show that Lys53 and Lys125 are critical components mediating this recognition event. Furthermore, our results demonstrate that a lysine residue in domain 1 is necessary, but not sufficient, for high-affinity binding by plasminogen.

It is well established that plasminogen exists in different conformations. During the process of plasminogen activation, cleavage of the Lys77−Lys78 bond in Glu-plasminogen releases the PAN module and generates a truncated plasminogen termed Lys-plasminogen. Formation of Lys-plasminogen is accompanied by a conformational change of Glu-plasminogen from a compact, closed α-conformation to a partially extended β-conformation with exposure of higher affinity LBS. The fourth kringle module mediates a second conformational change, from the β-conformation to the extended, open γ-conformation. In our previous studies on the generation of angiostatins from plasminogen, we have shown that these conformational changes can be mimicked *in vitro* by altering ion concentrations or incubation with benzamidine (*49*). Consistent with the predicted optimal exposure of plasminogen's LBS in the open conformation, our results demonstrate that Glu-plasminogen binds the N-terminal region of the CI-MPR with a 9-fold higher affinity in its open conformation compared to conditions (i.e., presence of Cl^- ions) that facilitate the closed conformation of Glu-plasminogen (K_d = 271 nM versus K_d = 20 nM, Figure 4).

Our studies have also shown that kringle 4 of plasminogen is required for high-affinity binding to the CI-MPR since the angiostatin containing kringles 1−4 of plasminogen, but not the angiostatin containing kringles 1−3, bound the CI-MPR with an affinity similar (within 2.4-fold) to that of full-length plasminogen (Table 2). A previous report which showed that the CI-MPR did not interact with kringle 4 alone absorbed to the surface of a 96-well plate (*32*) is consistent with our model (see below) that multiple kringle domains of plasminogen are involved in interacting with the N-terminal region of the CI-MPR. However, further studies are needed to rule out whether the nonspecific absorption of plasminogen's kringle 4 domain alone to the surface of a polystyrene well may have sterically masked the LBS of kringle 4. SPR analyses have shown that mini-plasminogen, which is comprised of kringle 5 and the C-terminal protease domain, bound the CI-MPR immobilized to a sensor chip with 5.4-fold higher affinity than plasminogen in the closed conformation formed in the presence of normal saline (K_d = ∼50 nM versus K_d = ∼270 nM), demonstrating that kringle 5 and/or the C-terminal protease domain of plasminogen are (is) capable of recognizing the CI-MPR (*32*). Given the diversity of interactions observed between plasminogen fragments and the CI-MPR *in vitro*, additional studies are needed to determine whether the CI-MPR plays a role *in vivo* to regulate the activity of certain angiostatins (i.e., K1−4, but not K1−3) via a mechanism analogous to its role in downregulating circulating levels of IGF-II in which the receptor targets this growth factor to the lysosome for degradation (*33*).

Much of the information regarding LBS specificity has been derived from studies using truncated forms of plasminogen and low molecular weight compounds, such as the zwitterioinic ligand AHA. These studies have shown that the kringles of plasminogen interact preferentially with proteins containing an exposed C-terminal lysine, such as that present in fibrinogen and fibrin fragments (*50*), as well as cell surface proteins including the annexin II S100A10 subunit (*51*). α_2-Antiplasmin contains a C-terminal lysine residue that is important for its interaction with isolated kringle domains (K1 and K4) (*52*), whereas an internal lysine residue appears to be involved in its interaction with intact plasmin/plasminogen (*53*). Some plasminogen binding molecules interact with a single LBS of plasminogen through multiple residues (e.g., at least one amino acid with a negatively charged side chain and one with a positively charged side chain) that mimic the charge properties of AHA. For example, three charged residues of tetranectin (Lys148, Glu150, and Asp165) are involved in its interaction with kringle 4 of plasminogen (*54*). Similarly, the LBS of plasminogen kringle 2 interacts electrostatically with Arg17, His18, Asp54, and Asp56 of the group A streptococcal M-like protein (PAM), VEK-30 (*55*). Acidic residues of the CI-MPR may also serve as key determinants recognized by plasminogen. Lys53 and Lys125 each have three adjacent acidic residues (carboxyl oxygen of Asp21, Asp51, and Asp 55 is 9.8, 4.2Å, and 11.7 Å, respectively, from the εN of Lys53; carboxyl oxygen of Glu384, Glu416, and Asp 418 is 11.8, 10.1, and 11.7 Å, respectively, from the εN of Lys125). Furthermore, Lys124, which is adjacent to Lys125 and is also solvent exposed (Figure 5), may also participate in plasminogen binding. Thus, a constellation of adjacent charged residues in the CI-MPR may also be involved in its high-affinity interaction with plasminogen.

The results presented in the current study, along with those of Leksa et al. (*32*), indicate that multiple regions of plasminogen interact with the CI-MPR. The CI-MPR may interact with multiple domains of plasminogen in a fashion similar to that described for streptokinase. Streptokinase binds plasminogen both through the protease domain, which involves wrapping of the N-terminal a, b, and g domains of streptokinase around the protease domain of plasminogen (*56*, *57*), and kringle 5 of plasminogen to a distinct site on the b domain of streptokinase (*58*). Our studies indicate that both Lys53 and Lys125 are required for high-affinity interaction with plasminogen (Table 3 and Figures 7 and 8). The observation that mutation of either Lys53 or Lys125 leads to a dramatic reduction in binding affinity (Table 3) indicates that a bidentate mode of interaction is required for plasminogen to bind tightly to the CI-MPR. It is also possible that plasminogen "samples" surface lysine residues other than Lys53 and Lys125, resulting in a low-affinity interaction with the receptor. This hypothesis is supported by analysis of binding interactions carried out at high concentrations of plasminogen in which a two-site binding model reveals low affinities (K_{d2} = 150−290 nM; Table 1). However, the possibility that the observation of a low-affinity binding interaction is due to a small fraction of Glu-plasminogen existing in the closed α-conformation cannot be ruled out. Lys53 and Lys125 are ∼60 Å apart on the surface of the CI-MPR. Although the structure of full-length plasminogen is not known, the crystal structure of K1−3 (*59*) indicates that the spacing of the two LBS from adjacent kringles is not sufficient to span this 60 Å distance between Lys53 and Lys125 of the CI-MPR. On the basis of our observation that K4 of plasminogen is essential for its interaction with the CI-MPR

(Table 2) and that K3 does not have a functional LBS, we propose that K1 and K4 of plasminogen participate in binding directly to Lys53 and Lys125 of the CI-MPR, which is consistent with the affinities of these two binding sites for AHA being 10−30 times higher than that of K2 (*3*−*6*) and the greater potential distance/flexibility between K1 and K4 versus that of K2 and K4 (*59*). Validation of this hypothesis to define the molecular basis of this high-affinity interaction will require further structural studies involving a complex between plasminogen and the N-terminal region of the CI-MPR.

One of the intriguing mechanisms of activation of plasminogen is through binding of not only the uPAR−uPA complex to the CI-MPR receptor but also the substrate plasminogen in which the CI-MPR functions to serve as a platform to concentrate plasminogen and its activator, uPA, on the cell surface (*19*). Our data are consistent with this model. Importantly, we show that the CI-MPR does not interact directly with uPA, which contains a kringle domain (Table 2), thus necessitating the CI-MPR's interaction with uPAR in order to bring uPA in close proximity to plasminogen bound to the CI-MPR. However, additional studies are needed to test this model and to define whether uPAR and plasminogen are able to bind simultaneously to the same CI-MPR molecule to facilitate plasminogen activation by uPA.

ACKNOWLEDGMENT

We thank Dr. Jung-Ja Kim for critical reading of the manuscript and Yoonyoung Go and Jackie Porath for protein purification and initial SPR analyses. The BIAcore 3000 instrument (Protein and Nucleic Acid Core Facility, Medical College of Wisconsin) was purchased through a grant from the Advancing a Healthier Wisconsin program.

SUPPORTING INFORMATION AVAILABLE

One figure showing the secondary structure and oligomeric state of Dom1His. This material is available free of charge via the Internet at http://pubs.acs.org.

REFERENCES

1. Tordai, H., Banyai, L., and Patthy, L. (1999) The PAN module: the N-terminal domains of plasminogen and hepatocyte growth factor are homologous with the apple domains of the prekallikrein family and with a novel domain found in numerous nematode proteins. *FEBS Lett. 461*, 63–67.
2. Castellino, F. J., and Ploplis, V. A. (2005) Structure and function of the plasminogen/plasmin system. *Thromb. Haemostasis 93*, 647–654.
3. Sehl, L. C., and Castellino, F. J. (1990) Thermodynamic properties of the binding of alpha-, omega-amino acids to the isolated kringle 4 region of human plasminogen as determined by high sensitivity titration calorimetry. *J. Biol. Chem. 265*, 5482–5486.
4. Hoover, G. J., Menhart, N., Martin, A., Warder, S., and Castellino, F. J. (1993) Amino acids of the recombinant kringle 1 domain of human plasminogen that stabilize its interaction with omega-amino acids. *Biochemistry 32*, 10936–10943.
5. Menhart, N., and Castellino, F. J. (1995) The importance of the hydrophobic components of the binding energies in the interaction of omega-amino acid ligands with isolated kringle polypeptide domains of human plasminogen. *Int. J. Pept. Protein Res. 46*, 464–470.
6. Nilsen, S. L., Prorok, M., and Castellino, F. J. (1999) Enhancement through mutagenesis of the binding of the isolated kringle 2 domain of human plasminogen to omega-amino acid ligands and to an internal sequence of a streptococcal surface protein. *J. Biol. Chem. 274*, 22380–22386.
7. Cao, Y., and Xue, L. (2004) Angiostatin. *Semin. Thromb. Hemostasis 30*, 83–93.
8. O'Reilly, M. S., Holmgren, L., Shing, Y., Chen, C., Rosenthal, R. A., Moses, M., Lane, W. S., Cao, Y., Sage, E. H., and Folkman, J. (1994) Angiostatin: a novel angiogenesis inhibitor that mediates the suppression of metastases by a Lewis lung carcinoma. *Cell 79*, 315–328.
9. Cao, Y., Ji, R. W., Davidson, D., Schaller, J., Marti, D., Sohndel, S., McCance, S. G., O'Reilly, M. S., Llinas, M., and Folkman, J. (1996) Kringle domains of human angiostatin. Characterization of the anti-proliferative activity on endothelial cells. *J. Biol. Chem. 271*, 29461–29467.
10. Cao, Y., Chen, A., An, S. S., Ji, R. W., Davidson, D., and Llinas, M. (1997) Kringle 5 of plasminogen is a novel inhibitor of endothelial cell growth. *J. Biol. Chem. 272*, 22924–22928.
11. Cao, R., Wu, H. L., Veitonmaki, N., Linden, P., Farnebo, J., Shi, G. Y., and Cao, Y. (1999) Suppression of angiogenesis and tumor growth by the inhibitor K1−5 generated by plasmin-mediated proteolysis. *Proc. Natl. Acad. Sci. U.S.A. 96*, 5728–5733.
12. Binder, B. R., Mihaly, J., and Prager, G. W. (2007) uPAR-uPA-PAI-1 interactions and signaling: a vascular biologist's view. *Thromb. Haemostasis 97*, 336–342.
13. Dass, K., Ahmad, A., Azmi, A. S., Sarkar, S. H., and Sarkar, F. H. (2008) Evolving role of uPA/uPAR system in human cancers. *Cancer Treat. Rev. 34*, 122–136.
14. Kornfeld, S. (1992) Structure and function of the mannose 6-phosphate/insulinlike growth factor II receptors. *Annu. Rev. Biochem. 61*, 307–330.
15. Dennis, P. A., and Rifkin, D. B. (1991) Cellular activation of latent transforming growth factor beta requires binding to the cation-independent mannose 6-phosphate/insulin-like growth factor type II receptor. *Proc. Natl. Acad. Sci. U.S.A. 88*, 580–584.
16. Tong, P. Y., Tollefsen, S. E., and Kornfeld, S. (1988) The cation-independent mannose 6-phosphate receptor binds insulin-like growth factor II. *J. Biol. Chem. 263*, 2585–2588.
17. Kang, J. X., Li, Y., and Leaf, A. (1997) Mannose-6-phosphate/insulin-like growth factor-II receptor is a receptor for retinoic acid. *Proc. Natl. Acad. Sci. U.S.A. 94*, 13671–13676.
18. Nykjaer, A., Christensen, E. I., Vorum, H., Hager, H., Petersen, C. M., Roigaard, H., Min, H. Y., Vilhardt, F., Moller, L. B., Kornfeld, S., and Gliemann, J. (1998) Mannose 6-phosphate/insulin-like growth factor-II receptor targets the urokinase receptor to lysosomes via a novel binding interaction. *J. Cell Biol. 141*, 815–828.
19. Godar, S., Horejsi, V., Weidle, U. H., Binder, B. R., Hansmann, C., and Stockinger, H. (1999) M6P/IGFII-receptor complexes urokinase receptor and plasminogen for activation of transforming growth factor-beta1. *Eur. J. Immunol. 29*, 1004–1013.
20. Olson, L. J., Yammani, R. D., Dahms, N. M., and Kim, J. J. (2004) Structure of uPAR, plasminogen, and sugar-binding sites of the 300 kDa mannose 6-phosphate receptor. *EMBO J. 23*, 2019–2028.
21. Brown, J., Delaine, C., Zaccheo, O. J., Siebold, C., Gilbert, R. J., van Boxel, G., Denley, A., Wallace, J. C., Hassan, A. B., Forbes, B. E., and Jones, E. Y. (2008) Structure and functional analysis of the IGF-II/IGF2R interaction. *EMBO J. 27*, 265–276.
22. Uson, I., Schmidt, B., von Bulow, R., Grimme, S., von Figura, K., Dauter, M., Rajashankar, K. R., Dauter, Z., and Sheldrick, G. M. (2003) Locating the anomalous scatterer substructures in halide and sulfur phasing. *Acta Crystallogr., Sect. D: Biol. Crystallogr. 59*, 57–66.
23. Reddy, S. T., Chai, W., Childs, R. A., Page, J. D., Feizi, T., and Dahms, N. M. (2004) Identification of a low affinity mannose 6-phosphate-binding site in domain 5 of the cation-independent mannose 6-phosphate receptor. *J. Biol. Chem. 279*, 38658–38667.
24. Hancock, M. K., Yammani, R. D., and Dahms, N. M. (2002) Localization of the carbohydrate recognition sites of the insulin-like growth factor II/mannose 6-phosphate receptor to domains 3 and 9 of the extracytoplasmic region. *J. Biol. Chem. 277*, 47205–47212.
25. Devi, G. R., Byrd, J. C., Slentz, D. H., and MacDonald, R. G. (1998) An insulin-like growth factor II (IGF-II) affinity-enhancing domain localized within extracytoplasmic repeat 13 of the IGF-II/mannose 6-phosphate receptor. *Mol. Endocrinol. 12*, 1661–1672.
26. Linnell, J., Groeger, G., and Hassan, A. B. (2001) Real time kinetics of insulin-like growth factor II (IGF-II) interaction with the IGF-II/mannose 6-phosphate receptor. The effects of domain 13 and pH. *J. Biol. Chem. 276*, 23986–23991.
27. Leksa, V., Godar, S., Cebecauer, M., Hilgert, I., Breuss, J., Weidle, U. H., Horejsi, V., Binder, B. R., and Stockinger, H. (2002) The N terminus of mannose 6-phosphate/insulin-like growth factor 2 receptor in regulation of fibrinolysis and cell migration. *J. Biol. Chem. 277*, 40575–40582.
28. Ghahary, A., Tredget, E. E., Mi, L., and Yang, L. (1999) Cellular response to latent TGF-beta1 is facilitated by insulin-like growth factor-II/mannose-6-phosphate receptors on MS-9 cells. *Exp. Cell Res. 251*, 111–120.

29. Ghahary, A., Tredget, E. E., Shen, Q., Kilani, R. T., Scott, P. G., and Houle, Y. (2000) Mannose-6-phosphate/IGF-II receptors mediate the effects of IGF-1- induced latent transforming growth factor beta 1 on expression of type I collagen and collagenase in dermal fibroblasts. *Growth Factors 17*, 167–176.
30. Munger, J. S., Harpel, J. G., Gleizes, P. E., Mazzieri, R., Nunes, I., and Rifkin, D. B. (1997) Latent transforming growth factor-beta—structural features and mechanisms of activation. *Kidney Int. 51*, 1376–1382.
31. Villevalois-Cam, L., Rescan, C., Gilot, D., Ezan, F., Loyer, P., Desbuquois, B., Guguen-Guillouzo, C., and Baffet, G. (2003) The hepatocyte is a direct target for transforming-growth factor beta activation via the insulin-like growth factor II/mannose 6-phosphate receptor. *J. Hepatol. 38*, 156–163.
32. Leksa, V., Godar, S., Schiller, H. B., Fuertbauer, E., Muhammad, A., Slezakova, K., Horejsi, V., Steinlein, P., Weidle, U. H., Binder, B. R., and Stockinger, H. (2005) TGF-beta-induced apoptosis in endothelial cells mediated by M6P/IGFII-R and mini-plasminogen. *J. Cell Sci. 118*, 4577–4586.
33. Oka, Y., Rozek, L. M., and Czech, M. P. (1985) Direct demonstration of rapid insulin-like growth factor II receptor internalization and recycling in rat adipocytes. Insulin stimulates ^{125}I-insulin-like growth factor II degradation by modulating the IGF-II receptor recycling process. *J. Biol. Chem. 260*, 9435–9442.
34. Ludwig, T., Eggenschwiler, J., Fisher, P., D'Ercole, A. J., Davenport, M. L., and Efstratiadis, A. (1996) Mouse mutants lacking the type 2 IGF receptor (IGF2R) are rescued from perinatal lethality in Igf2 and Igf1r null backgrounds. *Dev. Biol. 177*, 517–535.
35. Valenzano, K. J., Remmler, J., and Lobel, P. (1995) Soluble insulin-like growth factor II/mannose 6-phosphate receptor carries multiple high molecular weight forms of insulin-like growth factor II in fetal bovine serum. *J. Biol. Chem. 270*, 16441–16448.
36. Marron-Terada, P. G., Hancock, M. K., Haskins, D. J., and Dahms, N. M. (2000) Recognition of *Dictyostelium discoideum* lysosomal enzymes is conferred by the amino-terminal carbohydrate binding site of the insulin-like growth factor II/mannose 6-phosphate receptor. *Biochemistry 39*, 2243–2253.
37. Reddy, S. T., and Dahms, N. M. (2002) High-level expression and characterization of a secreted recombinant cation-dependent mannose 6-phosphate receptor in *Pichia pastoris*. *Protein Expression Purif. 26*, 290–300.
38. Marron-Terada, P. G., Bollinger, K. E., and Dahms, N. M. (1998) Characterization of truncated and glycosylation-deficient forms of the cation-dependent mannose 6-phosphate receptor expressed in baculovirus-infected insect cells. *Biochemistry 37*, 17223–17229.
39. Myszka, D. G. (2000) Kinetic, equilibrium, and thermodynamic analysis of macromolecular interactions with BIACORE. *Methods Enzymol. 323*, 325–340.
40. Kiess, W., Greenstein, L. A., White, R. M., Lee, L., Rechler, M. M., and Nissley, S. P. (1987) Type II insulin-like growth factor receptor is present in rat serum. *Proc. Natl. Acad. Sci. U.S.A. 84*, 7720–7724.
41. Causin, C., Waheed, A., Braulke, T., Junghans, U., Maly, P., Humbel, R. E., and von Figura, K. (1988) Mannose 6-phosphate/insulin-like growth factor II-binding proteins in human serum and urine. Their relation to the mannose 6-phosphate/insulin-like growth factor II receptor. *Biochem. J. 252*, 795–799.
42. MacDonald, R. G., Tepper, M. A., Clairmont, K. B., Perregaux, S. B., and Czech, M. P. (1989) Serum form of the rat insulin-like growth factor II/mannose 6-phosphate receptor is truncated in the carboxyl-terminal domain. *J. Biol. Chem. 264*, 3256–3261.
43. Xu, Y., Papageorgiou, A., and Polychronakos, C. (1998) Developmental regulation of the soluble form of insulin-like growth factor-II/mannose 6-phosphate receptor in human serum and amniotic fluid. *J. Clin. Endocrinol. Metab. 83*, 437–442.
44. Olson, L. J., Dahms, N. M., and Kim, J. J. (2004) The N-terminal carbohydrate recognition site of the cation-independent mannose 6-phosphate receptor. *J. Biol. Chem. 279*, 34000–34009.
45. Tong, P. Y., and Kornfeld, S. (1989) Ligand interactions of the cation-dependent mannose 6-phosphate receptor. Comparison with the cation-independent mannose 6-phosphate receptor. *J. Biol. Chem. 264*, 7970–7975.
46. MacDonald, R. G., Pfeffer, S. R., Coussens, L., Tepper, M. A., Brocklebank, C. M., Mole, J. E., Anderson, J. K., Chen, E., Czech, M. P., and Ullrich, A. (1988) A single receptor binds both insulin-like growth factor II and mannose-6-phosphate. *Science 239*, 1134–1137.
47. Marshall, J. M., Brown, A. J., and Ponting, C. P. (1994) Conformational studies of human plasminogen and plasminogen fragments: evidence for a novel third conformation of plasminogen. *Biochemistry 33*, 3599–3606.
48. Urano, T., Sator de Serrano, V., Chibber, B. A., and Castellino, F. J. (1987) The control of the urokinase-catalyzed activation of human glutamic acid 1-plasminogen by positive and negative effectors. *J. Biol. Chem. 262*, 15959–15964.
49. Warejcka, D. J., and Twining, S. S. (2005) Specific conformational changes of plasminogen induced by chloride ions, 6-aminohexanoic acid and benzamidine, but not the overall openness of plasminogen regulate, production of biologically active angiostatins. *Biochem. J. 392*, 703–712.
50. Doolittle, R. F. (2008) Searching for differences between fibrinogen and fibrin that affect the initiation of fibrinolysis. *Cardiovasc. Hematol. Agents Med. Chem. 6*, 181–189.
51. MacLeod, T. J., Kwon, M., Filipenko, N. R., and Waisman, D. M. (2003) Phospholipid-associated annexin A2-S100A10 heterotetramer and its subunits: characterization of the interaction with tissue plasminogen activator, plasminogen, and plasmin. *J. Biol. Chem. 278*, 25577–25584.
52. Frank, P. S., Douglas, J. T., Locher, M., Llinas, M., and Schaller, J. (2003) Structural/functional characterization of the alpha 2-plasmin inhibitor C-terminal peptide. *Biochemistry 42*, 1078–1085.
53. Wang, H., Yu, A., Wiman, B., and Pap, S. (2003) Identification of amino acids in antiplasmin involved in its noncovalent "lysine-binding-site"-dependent interaction with plasmin. *Eur. J. Biochem. 270*, 2023–2029.
54. Graversen, J. H., Jacobsen, C., Sigurskjold, B. W., Lorentsen, R. H., Moestrup, S. K., Thogersen, H. C., and Etzerodt, M. (2000) Mutational analysis of affinity and selectivity of kringle-tetranectin interaction. Grafting novel kringle affinity ontp the trtranectin lectin scaffold. *J. Biol. Chem. 275*, 37390–37396.
55. Rios-Steiner, J. L., Schenone, M., Mochalkin, I., Tulinsky, A., and Castellino, F. J. (2001) Structure and binding determinants of the recombinant kringle-2 domain of human plasminogen to an internal peptide from a group A streptococcal surface protein. *J. Mol. Biol. 308*, 705–719.
56. Wang, X., Lin, X., Loy, J. A., Tang, J., and Zhang, X. C. (1998) Crystal structure of the catalytic domain of human plasmin complexed with streptokinase. *Science 281*, 1662–1665.
57. Loy, J. A., Lin, X., Schenone, M., Castellino, F. J., Zhang, X. C., and Tang, J. (2001) Domain interactions between streptokinase and human plasminogen. *Biochemistry 40*, 14686–14695.
58. Tharp, A. C., Laha, M., Panizzi, P., Thompson, M. W., Fuentes-Prior, P., and Bock, P. E. (2009) Plasminogen substrate recognition by the streptokinase-plasminogen catalytic complex is facilitated by Arg253, Lys256, and Lys257 in the streptokinase {beta}-domain and kringle 5 of the substrate. *J. Biol. Chem. 284*, 19511–19521.
59. Abad, M. C., Arni, R. K., Grella, D. K., Castellino, F. J., Tulinsky, A., and Geiger, J. H. (2002) The X-ray crystallographic structure of the angiogenesis inhibitor angiostatin. *J. Mol. Biol. 318*, 1009–1017.
60. DeLano, W. L. (2002) The PyMOL Molecular Graphics System, DeLano Scientific LLC, San Carlos, CA.